

Numerical Simulation of a Vessel's Manoeuvring Performance in Regular Waves

Christos Pollalis^a, Dimitrios Mourkogiannis^b, Evangelos Boulougouris^c

^a *Maritime Risk Group, National Technical University of Athens, Greece*

^b *National Technical University of Athens, Greece*

^c *Maritime Safety Research Center, University of Strathclyde, United Kingdom*

Abstract

The present paper deals with the numerical simulation of ship's manoeuvring performance in regular waves. This is made possible by employing the time-domain code ELIGMOS which adopts a hybrid formulation in order to couple seakeeping and manoeuvring contributions. First and steady second-order wave-induced forces are incorporated, implementing a multidimensional interpolation scheme in order to account for their dependency on the instantaneous heading and forward speed values. Two methods have been adopted for the calculation of the added resistance regarding the size of the wavelength (short or long wave seas), namely a far and a near-field one, using the hydrodynamic software NEWDRIFT+ and NEWDRIFT v.7. Low frequency hydrodynamic manoeuvring forces are incorporated by adopting the expressions suggested by the Japanese MMG (Manoeuvring Modelling Group) method. Validation of the suggested methodology is attempted through the comparison of numerical simulations of turning circle tests in calm water and in regular waves with available experimental evidence for the S-175 container ship.

1. INTRODUCTION

Numerical prediction of the manoeuvring performance of a ship at her design stage and in calm water conditions is a common practice nowadays. Relevant models have been developed which offer that possibility with satisfactory agreement. They consist of a practical alternative to the costly and time-consuming experiments. The aforementioned models can be separated in two groups, namely the whole or Abkowitz-type models (Abkowitz, 1964) and the modular-type ones (Yasukawa and Yoshimura, 2015). However, a ship hardly

ever operates in such environmental conditions. Instead, most of a marine vessel's manoeuvres are performed in real conditions, namely under the presence of waves and other environmental actions (i.e. wind and current). Therefore, the incorporation of such external forces is mandatory in order to establish realistic models, capable of assessing a marine vessel's manoeuvrability in adverse weather conditions.

Numerical prediction of ship manoeuvring in waves has been an attractive field of study for naval architects since the 1980s when the first

experiments and numerical simulations took place (Hirano et al., 1980). Since that time, several efforts have been made in order to experimentally investigate a vessel's manoeuvrability in regular (Ueno et al., 2003, Yasukawa and Nakayama, 2009) and irregular seas (Yasukawa, 2006).

More recently, results concerning the experimental investigation of the DTC (Duisburg Test Case) manoeuvrability in waves were conducted within the framework of FP7 EU research project SHOPERA (Energy Efficient Safe Ship OPERATION). The main objective of the aforementioned project was to suggest criteria regarding the sufficiency in power requirements and steering devices for safe marine operations in adverse weather conditions. The cause were the concerns regarding the implications caused by the introduction of the EEDI (Energy Efficiency Design Index) for new ships in 2012 (MEPC.212(63)). In this context, the performed experimental studies provided valuable outcome to researchers who attempt to validate their numerical codes in order to be capable of accurately simulating the behaviour of a manoeuvring vessel in waves. In general, the available methodologies couple the manoeuvring theory used to describe the zero-frequency motion of a marine vessel in calm water and the seakeeping theory that describes the motion of a ship in waves, usually referring at a specific forward speed. Coupling of the aforementioned theories in the time-domain is valid under the principle of linear superposition (Denis and Pierson, 1953).

Such time-domain software is grouped in two categories: The two-time scale (e.g. Hirano et al., 1980, Chroni et al., 2015) and the hybrid

one (e.g. Fang et al., 2005). The former, separates seakeeping and manoeuvring approaches as the high and the low frequency one, which are solved separately, whilst ship motions are superimposed at the end of the time increment. Starting from the solution of the manoeuvring problem, interconnection between the two modules is performed at defined time steps where certain criteria are met (e.g. the increment of the vessel's yaw angle $\Delta\psi$ reaches a specific value, Skejic and Faltinsen, 2008). At this moment, the actual forward speed and heading angle, determined by the solution of the manoeuvring problem, are passed as input parameters to the seakeeping calculations. As it concerns the hybrid method, seakeeping and manoeuvring-related force components are blended at a common system of mathematical equations, which is solved at the same time step. In any case, a crucial aspect that affects the accurate evaluation of a marine vessel's manoeuvrability in waves is the incorporation of the steady second-order wave forces. When dealing with the horizontal ship motions (surge-sway-yaw), the aforementioned refer to the added resistance, the sway and yaw drift forces, which depend on the instantaneous forward speed and heading angle.

Starting from Hirano's et al. (1980) pioneering work, where the two-time scale approach was adopted, the incorporation of steady second-order wave forces is documented as a crucial aspect for the accurate simulation of a vessel's manoeuvring performance in waves. However, a drawback of their methodology is that the forward speed effect on the calculation of the mean second-order forces

was not taken into consideration. In the work of Skejic and Faltinsen (2008), after a brief review regarding the best option among four methods developed for the calculation of mean second-order forces in relation to the size of the wavelength, it is concluded that for wavelength equal to the ship's length ($\lambda/L=1$), Faltinsen et al.'s (1980) method should be adopted. The latter, is suitable for slender as well as full hull forms, whereas it can be used for the calculation of all force components related with the vessel's horizontal motion with satisfactory accuracy. Fossen (2005) delivered an explanatory study on ship manoeuvring in waves, providing the mathematical background about the necessary transformation among the various reference frames. The solution he presented is based on a two-time scale approach, whereas a state-space approach was adopted for the calculation of the damping forces. Another study on ship manoeuvrability in regular waves adopting the two-time scale method was published by Seo and Kim (2011) who coupled a 4-DOF manoeuvring module with a 6-DOF linear seakeeping one. Good agreement against experimental results is observed concerning the manoeuvring performance of the S-175 container ship in head waves and in case where the wavelength was equal or greater than the ship's length, proving that a direct pressure integration scheme for the calculation of the steady second-order forces, as this proposed by Faltinsen (1980), is appropriate in such conditions. Similar to the aforementioned results were also derived from Zhang et al. (2017), predicting ship's manoeuvrability in regular waves with better accuracy when $\lambda/L=1$ and waves initially formed an angle of

180° with the vessel's longitudinal axis (head waves). As a mean to perform numerical simulations in shorter wavelength to ship length ratio ($\lambda/L=0.5$), the implementation of a far field method (Liu et al., 2011) instead of a direct pressure integration one is more appropriate for the calculation of the added resistance as it is suggested in Chroni et al. (2015). Such environmental condition is of high practical interest nowadays as the size of marine vessels is continuously increasing. An improvement of Chroni et al. method was presented in Fournarakis et al. (2016), where CFD (Computational Fluid Dynamics) simulations were utilized in order to compute the manoeuvring derivatives by means of virtual CMT (Circular Motion Tests), avoiding costly and time-consuming experiments. Further improvement of the two-time scale method was attained from Subramanian and Beck (2015) who developed a 2D body-exact method for simulating the seakeeping contributions, allowing the incorporation of nonlinear forces taking part in large amplitude waves.

Modelling of ship's manoeuvrability in waves implementing a hybrid approach was initially met in the work of Hamamoto and Kim (1993) and Hamamoto and Saito (1992). The major development in these studies concerns the introduction of a new coordinate system (the so-called Horizontal Body-Fixed Reference Frame), which allows the coupling of manoeuvring and seakeeping modules even in case of large waves. Nonlinearity in wave-induced forces concerned the two major contributions, namely the Froude-Krylov and restoring ones. In the following years, utilisation of the aforementioned reference frame in order to account for wave

force nonlinearities is documented in the works of several researchers, like Fang et al. (2005) and Ayaz et al. (2006). The calculation of radiation and diffraction forces consists of the major difference between these two numerical models since Ayaz et al. considered the variation of added masses and damping coefficients every 10° of the heading angle, whilst Fang et al. account for these terms through encounter frequency-dependent coefficients. However, both methods neglect the effect of the steady second-order forces, a fact that introduces substantial inaccuracies to the presented results especially after the first 360° of the turning trajectory. Sutulo and Soares (2006) study on ship manoeuvrability in waves included the roll response of S-175 during turning motion, which took larger values than in straight course. The latter revealed the augmented effect of seakeeping and manoeuvring coupling on roll angle. Use of the 2D strip theory restricted the applicability of the discussed method to slender or slowly sailing ships. More recently, Ghillece and Moctar (2018) presented a 6-DOF nonlinear model for ship manoeuvring in regular waves accounting only for the steady second-order wave forces. The latter were evaluated by means of reliable RANSE (Raynolds-Averaged Navier Stokes Equations) solvers that give good results for short as well as long wavelengths. Comparison with experimental results concerning the turning motion of the DTC in short ($\lambda/L=0.5$) and moderate ($\lambda/L=0.68$) wavelengths show good agreement in case of low and higher wave height ($H=2\text{m}$ and $H=4\text{m}$).

In a recent article (Yao et al., 2021), a novel methodology was proposed for simulating a

ship's turning performance in regular waves, solving the pure low-frequency equations. The angular motion amplitudes were predicted by solving the pure high-frequency equations derived after subtracting the pure low-frequency equation from the transient ones. The formation of the pure low-frequency ship motion equations was succeeded by considering the wave-induced mean inertial forces and moments as well. Such formulation is suggested in case where the wave amplitude is large enough. The major improvements introduced by their study is that the mean inertial forces and moments originated by the second-order wave motions have been retained, whilst the longitudinal speed effect has been taken into consideration within the proposed modelling approach.

The main contribution of the present research work is the incorporation of a numerical scheme that allows the calculation of first and second-order wave forces in an effective multidimensional interpolation scheme. This led to the development of a novel hybrid time-domain approach, capable of capturing quite accurately the manoeuvring performance of a vessel in waves.

2. METHODOLOGY

The present methodology is based on a hybrid time-domain approach, where the assessment of a vessel's manoeuvrability in regular waves is performed through the numerical solution of a single system of equations including surge-sway and yaw motions. The external forces consist of first and steady second-order ones, whereas a third-order Taylor expansion is adopted in order to account for the hydrodynamic loads

originated from the ship's manoeuvring motion in calm water. Oscillatory and mean wave forces are considered functions of the vessel's forward speed and heading angle. Due to this consideration, their incorporation is performed implementing the general Newton's interpolation scheme (Dahlquist and Björck, 2003) on their pre-calculated frequency-domain values. Propeller and rudder forces are modeled adopting the relevant MMG formulae (Yasukawa and Yoshimura, 2015). Sea environment is modelled considering small amplitude waves having short ($\lambda/L=0.5$) to large ($\lambda/L=1.0$) wavelength compared with the ship's length.

2.1 System of equations

The equations of ship motion have been formulated with respect to the body-fixed reference frame (oxyz) that follows the slowly varying path of the turning ship. Applying the necessary transformations, ship position and yaw angle are expressed at the inertial coordinate system (OXYZ) which coincides with the vessel's starting point at $t=0$. The aforementioned reference frames are depicted in Fig. 1, whilst the panel geometry of S-175 is illustrated in Fig. 2.

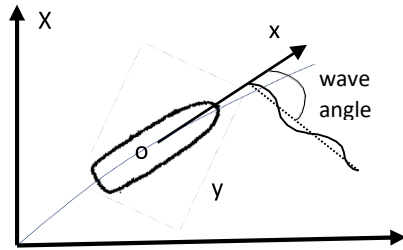


Figure 1. Coordinate systems

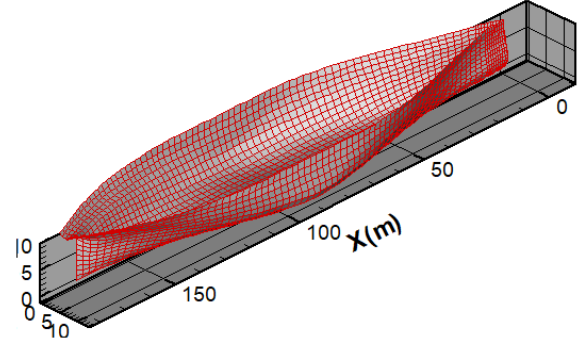


Figure 2. Panel geometry of S-175

Based on the description given above, the equations of motion in surge-sway and yaw are illustrated below:

$$\text{Surge: } (M + M_x)\ddot{u} = X_{FK} + X_{DIFF} + X_{AR} + X_{HD} + X_R + (1 - t)T - R \quad (3.1)$$

$$\text{Sway: } (M + M_y)\ddot{v} + M_{X_G}\ddot{r} = Y_{FK} + Y_{DIFF} + Y_{HD} + Y_{DF} + Y_R \quad (3.2)$$

$$\text{Yaw: } (I_{zz} + J_{zz})\ddot{r} + M_{X_G}\ddot{v} = N_{FK} + N_{DIFF} + N_{HD} + N_{DF} + N_R \quad (3.3)$$

In Equations (3.1)-(3.3) u, v, r refer to surge, -sway and yaw velocities and the subscripts FK, DIFF, HD, T, R denote the Froude-Krylov, diffraction, hydrodynamic thrust and rudder forces, whereas AR, DF indicate the steady added resistance and drift forces. Additionally, M, I_{zz} stand for the ship's mass and moment of inertia about her vertical axis, whilst $M_x, M_y,$ and J_{zz} are the added masses and added moment of inertia with respect to the body-fixed axes respectively.

Detailed presentation of the process followed to calculate each force component is illustrated in the following paragraphs.

2.2 Seakeeping-related forces

3.2.1 First-order wave forces

The complex amplitudes and phase angles of the first-order wave forces (Froude-Krylov and Diffraction) have been calculated adopting a 3D panel method (Papanikolaou and Schelling, 1992) which assumes potential flow characteristics. According to this, the velocity potential can be decomposed into a steady (S) and a time dependent (T) part as indicated below.

$$\Phi(x, y, z; t) = -Ux + \Phi_S(x, y, z) + \Phi_T e^{-i\omega t} \quad (3.4)$$

Further decomposition of the unsteady potential leads to the following expression where quantities at the RHS refer to incident, diffracted and radiation potentials.

$$\Phi_T = \Phi_I + \Phi_D + \sum_{j=1}^6 \xi_j \Phi_{R,j} \quad (3.5)$$

In Eq. (3.5), the incident potential for small amplitude waves can be expressed using the following formula (Papanikolaou, 1985):

$$\Phi_I = \frac{1}{k} \frac{\cosh k_0(z+d)}{\cosh k_0 d} e^{ik_0(x \cos \beta + y \sin \beta)} \quad (3.6)$$

In the aforementioned expression, d stands for the sea depth, β is the angle of the ship relative to the wave's direction and k is the frequency number that can be expressed by the dispersion relationship depicted in Eq. (3.7).

$$k = k_0 \tanh k_0 d \quad (3.7)$$

The continuity equation as well as the following boundary conditions must be fulfilled for all the potentials φ_i ($i=0, \dots, 7$) in the fluid domain:

$$\nabla^2 \varphi_i = 0, \text{ Laplace equation} \quad (3.8)$$

$$-\omega^2 \varphi_i + g \frac{\partial \varphi_i}{\partial z} = 0, \text{ linearized boundary condition on the free surface } z=0 \quad (3.9)$$

$$\frac{\partial \varphi_i}{\partial z} = 0, \text{ on the sea bed } z=-d \quad (3.10)$$

Additionally, the motion potentials φ_i ($i=1, \dots, 6$) and the diffraction should satisfy the following kinematic body boundary condition:

$$\begin{aligned} \frac{\partial \varphi_i}{\partial \vec{n}} &= n_i \\ \frac{\partial \varphi_D}{\partial \vec{n}} &= -\frac{\partial \varphi_I}{\partial \vec{n}} \end{aligned} \quad (3.11)$$

In the last equation, \vec{n} is the unit normal vector on the body surface pointing outwards.

The incorporation of the first-order wave forces in the time-domain model is performed by implementing the following expression (Fonseca and Soares, 1998):

$$F(t) = \text{Re}\{(F_I(u, \beta) + F_D(u, \beta))e^{i\omega_e t}\} \quad (3.12)$$

As indicated in Eq. (3.12), the values of the first-order forces F_I (Froude-Krylov) and F_D (Diffraction) are determined by implementing a multidimensional interpolation scheme with respect to the vessel's instantaneous longitudinal speed and heading angle. More details can be found in paragraph 3.2.3.

3.2.2 Mean second-order wave forces

In the present analysis, where ship manoeuvring motion is investigated with respect to the horizontal X-Y plane, the steady second-order forces originated by the presence of the waves consist of the added resistance, the sway and yaw drift forces.

Two methods that are based on the potential theory are available in order to calculate the aforementioned forces.

The first one, or the so-called far-field method (e.g. Maruo (1960), Liu (2011)), is using the first-order potential and the Kochin functions concept. According to Maruo's (1963) formulation, the following expression can be used for the calculation of the added resistance.

$$R_{AW} = \frac{\rho}{8\pi} \left(\int_{-\pi/2}^{\alpha_0} + \int_{\alpha_0}^{\pi/2} - \int_{\pi/2}^{3\pi/2} \right) |H(k_1, \theta)|^2 \cdot \frac{k_1(k_1 \cos \theta - k \cos \chi)}{\sqrt{1-4\Omega \cos \theta}} d\theta + \frac{\rho}{8\pi} \int_{\alpha_0}^{2\pi-\alpha_0} |H(k_2, \theta)|^2 \cdot \frac{k_2(k_2 \cos \theta - k \cos \chi)}{\sqrt{1-4\Omega \cos \theta}} d\theta \quad (3.13)$$

In Eq. (3.13), ρ is the density of the water, α_0 is the critical angle, Ω is the so-called Hanaoka parameter ($\Omega = \omega_e U/g$) and $H(k_j, \theta)$ are the Kochin functions. In addition, θ is the angle of the elementary waves that are generated by the vessel and χ is the heading angle with respect to the incident wave. Faltinsen et al. (1980) proposed the following asymptotic formula (Eq. 3.15) for the calculation of the added resistance in case of short waves assuming a total reflection of the incident wave over the body's non-shaded area.

$$F_1 = \int_L \bar{F}_n \sin \varphi dl \quad (3.14)$$

$$\bar{F}_n = \frac{1}{2} \rho g \zeta_a^2 \left\{ \sin^2(\varphi - \chi) + \frac{2\omega U}{g} \left[1 + \cos \varphi \cos(\varphi - \chi) \right] \right\} \quad (3.15)$$

In Eq. 3.15, ω is the wave's circular frequency and U means the vessel's forward speed. The previously described method, which is incorporated in the software

NEWDRIFT+, has been utilised for the calculation of the added resistance in case where $\lambda/L=0.5$. For medium to large wavelengths (i.e. $\lambda/L=0.7, 1.0$ and 1.2) the mean second-order wave forces have been calculated with respect to a near-field method, which adopts a direct pressure integration scheme over the wetted portion of the ship's hull (Papanikolaou and Zaraphonitis, 1987). The aforementioned methodology is implemented through the hydrodynamic software NEWDRIFT v.7.

3.2.3 Multidimensional interpolation scheme

It was mentioned previously that the first and second-order wave forces have been calculated for several speed and heading values. More specifically, the aforementioned forces have been calculated for 4 speeds (corresponding to $F_n=0, 0.05, 0.10$ and 0.15) and 18 equally spaced angle increments (from 0° to 180°). A practical scheme is employed afterwards (Pollalis and Boulougouris, 2021) in order to incorporate the aforementioned forces during the numerical simulations. This was achieved by adopting the general Newton's interpolation rule (Dahlquist and Björck, 2003). According to this method, given the instantaneous heading, the values of the force with respect to the 4 different forward speeds are determined, i.e. $F_1(\beta_{inst}), F_2(\beta_{inst}), F_3(\beta_{inst})$ and $F_4(\beta_{inst})$. Then, the final interpolated value with respect to the exact forward speed value is determined using the following expressions:

$$\mu_1 = \frac{F_2(\beta_{inst}) - F_1(\beta_{inst})}{u_2 - u_1} \quad (3.16)$$

$$\mu_2 = \frac{F_3(\beta_{inst}) - 2 \cdot F_2(\beta_{inst}) + F_1(\beta_{inst})}{(u_2 - u_1)(u_3 - u_1)} \quad (3.17)$$

$$\mu_3 = \frac{F_4(\beta_{inst}) - 3 \cdot F_3(\beta_{inst}) + 3 \cdot F_2(\beta_{inst}) - F_1(\beta_{inst})}{(u_2 - u_1)(u_3 - u_1)(u_4 - u_1)} \quad (3.18)$$

2.3 Manoeuvring-related forces

According to the Japanese MMG model, the manoeuvring-related forces are computed in distinct modules that concern the hydrodynamic (hull) forces, the propeller and the rudder forces. The formulation followed in the present simulations is depicted below.

3.3.1 Hydrodynamic (hull) forces

In order to calculate the hydrodynamic forces exerted on the vessel's naked hull due to the slow-varying manoeuvring motion, a 3rd order Taylor expansion has been adopted.

The latter, incorporates linear and nonlinear with regards to surge, sway, yaw and cross coupling nondimensional velocities and drift angle β as it can be seen below (Sano and Yasukawa, 2008).

$$X'_{HD} = X'_{\beta\beta}\beta'^2 + X'_{\beta r}\beta'r' + X'_{rr}r'^2 \quad (3.19)$$

$$Y'_{HD} = Y'_{\beta}\beta' + Y'_{r}r' + Y'_{\beta\beta\beta}\beta'^3 + Y'_{\beta\beta r}\beta'^2r' + Y'_{\beta rr}\beta'r'^2 + Y'_{rrr}r'^3 \quad (3.20)$$

$$N'_{HD} = N'_{\beta}\beta' + N'_{r}r' + N'_{\beta\beta\beta}\beta'^3 + N'_{\beta\beta r}\beta'^2r' + N'_{\beta rr}\beta'r'^2 + N'_{rrr}r'^3 \quad (3.21)$$

The nondimensional manoeuvring derivatives that appear in Eqs. (3.19-3.21) have been experimentally determined. The dimensional values of the hydrodynamic (hull) forces that appear in Eqs. (3.1)-(3.3)

have been obtained by multiplying with $0.5\rho LTU^2$, whilst the dimensional yaw moment with $0.5\rho L^2TU^2$. In the aforementioned expressions T, U stand for the vessel's draught and forward speed respectively.

3.3.2 Propeller force

According to the MMG model the thrust force induced by the propeller can be calculated using the following formula:

$$T = \rho n_p^2 D_p^4 K_T(J_p) \quad (3.22)$$

In Eq. (3.22) n_p means the propeller revolutions per second, D is the propeller's diameter, K_T stands for the thrust coefficient and J_p is the propeller's advance coefficient which can be calculated using the following expression:

$$J_p = \frac{u(1-w_p)}{n_p D_p} \quad (3.23)$$

The aforementioned coefficient encompasses the reduction of the axial flow speed to the propeller due to the presence of the wake. This is shown by the introduction of the wake fraction coefficient $(1-w_p)$. The coefficient w_p changes with the drift angle as it is indicated by the following expression.

$$w_p = w_{p0} e^{(C_1 \beta_p^2)} \quad (3.24)$$

where w_{p0} is the wake fraction at zero drift angle, $C_1 = -8$ is the correction factor and β_p is the drift angle at the propeller's position.

3.3.3 Rudder forces

A rudder's angular deflection δ generates forces in surge (X_R), sway (Y_R) directions and a yaw moment (N_R) about the vessel's centre

of gravity. According to the MMG model, the aforementioned can be calculated through the following expressions:

$$X_R = -(1 - t_R)FN\sin\delta \quad (3.25)$$

$$Y_R = -(1 + a_H)FN\cos\delta \quad (3.26)$$

$$N_R = -(x_R + a_H x_H)FN\cos\delta \quad (3.27)$$

In the expressions shown above, FN means the normal force generated on the rudder's area A_R which is equal to

$$FN = \frac{1}{2}\rho A_R f_a U_R^2 \sin a_R \quad (3.28)$$

In the latter, f_a is the lift coefficient's gradient of the rudder and can be estimated using the Fujii's formula (Fujii and Tuda, 1961). U_R and a_R mean the flow velocity and rudder's effective inflow angle respectively. In the present analysis they have been calculated according to the following formulae:

$$U_R = \sqrt{u_R^2 + v_R^2} \quad (3.29)$$

$$a_R = \delta - \arctan\left(\frac{v_R}{u_R}\right) \quad (3.30)$$

The flow's axial (u_R) and transverse (v_R) velocities at rudder's position can be determined implementing the following expressions (Sano and Yasukawa, 2008):

$$u_R = \varepsilon u (1 - w_p) \cdot \sqrt{\eta \left[1 + \frac{k_x}{\varepsilon} \left(\sqrt{1 + \frac{8K_T}{\pi J_p^2}} - 1 \right) \right] + (1 - \eta)} \quad (3.28)$$

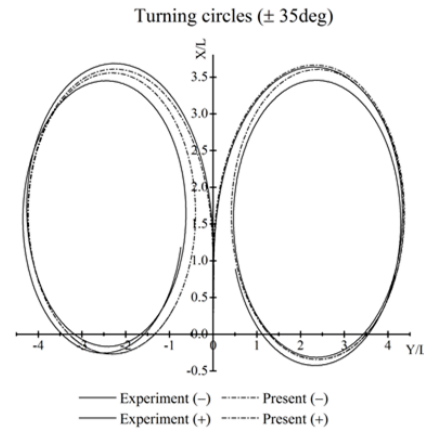
$$v_R = U_{YR} \beta_R \quad (3.29)$$

In the last two expressions $\eta = D_p/H_R$ (ratio of propeller diameter over rudder's height), $\varepsilon = (1 - w_R)/(1 - w_p)$ and k_x is the acceleration

rate which take the value of 0.8, 0.921 and 0.631 respectively. Further, γ_R means the flow straightening coefficient which equals to 0.193 and 0.088 for starboard and port turning maneuvers respectively. Finally, β_R is the drift angle at the position of the rudder.

3. RESULTS

In this section, starboard and port turning circles ($\delta = \pm 35^\circ$) of S-175 initially in calm water and then in head and beam small amplitude waves ($\zeta_a = 1\text{m}$) are presented. The vessel's manoeuvrability is examined in small ($\lambda/L = 0.5$) to large ($\lambda/L = 1.0$) regular waves. Together with the derived trajectories, comparison of the time histories of surge and yaw velocities are depicted as well.



Comparison of the present methodology with available experimental data in calm water is excellent as it is illustrated in Fig. 3. Valid results in calm water is a prerequisite and a good starting point for the validation process of a time-domain software that allows its coupling with the seakeeping terms.

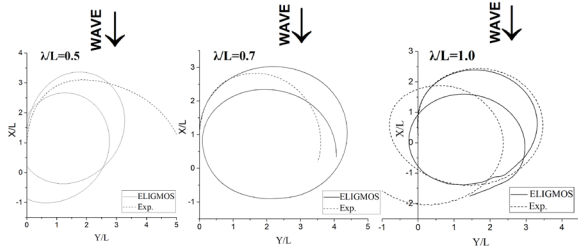


Figure 4. Starboard turning circles of S-175 in regular head waves

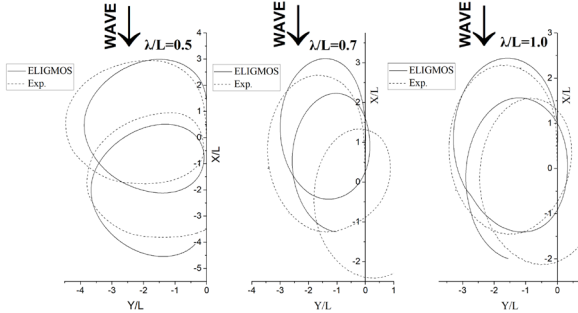


Figure 5. Port turning circle of S-175 in head waves

The time histories of surge velocity and yaw rate for the turning circles presented above is illustrated in Figs. 6 and 7.

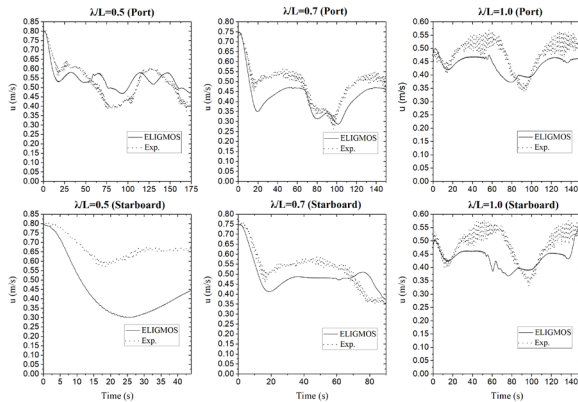


Figure 6. Comparison of surge velocity during port and starboard turning circles in regular head waves

Similar figures depicting the vessel's manoeuvrability and fluctuation of the longitudinal and yaw velocities in regular beam waves are presented below.

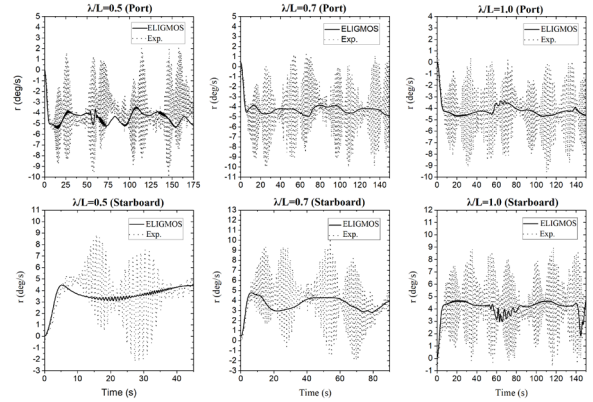


Figure 7. Comparison of yaw rate during port and starboard turning circles in regular head waves

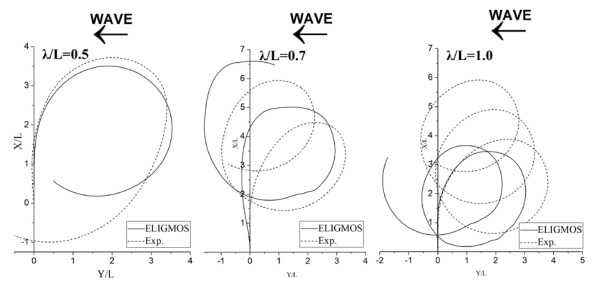


Figure 8. Starboard turning circles of S-175 in regular beam waves

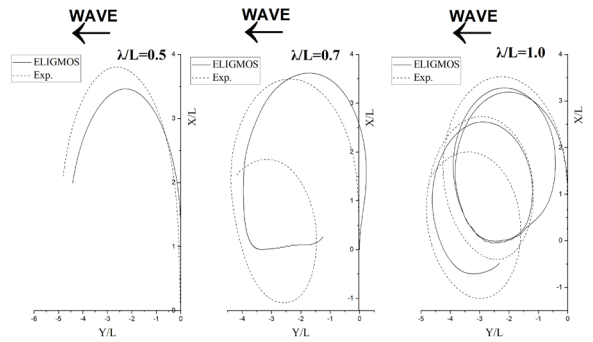


Figure 9. Port turning circle of S-175 in beam waves

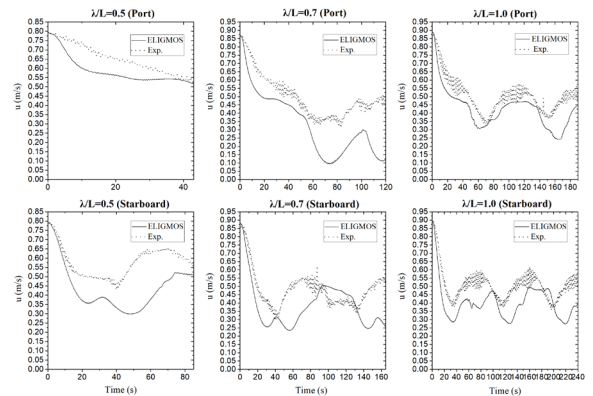


Figure 10. Comparison of surge velocity during port and starboard turning circles in regular beam waves

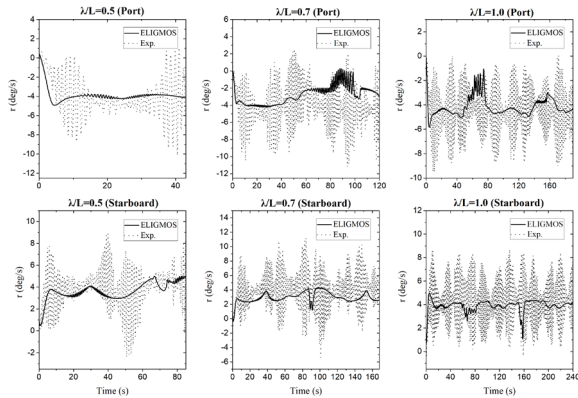
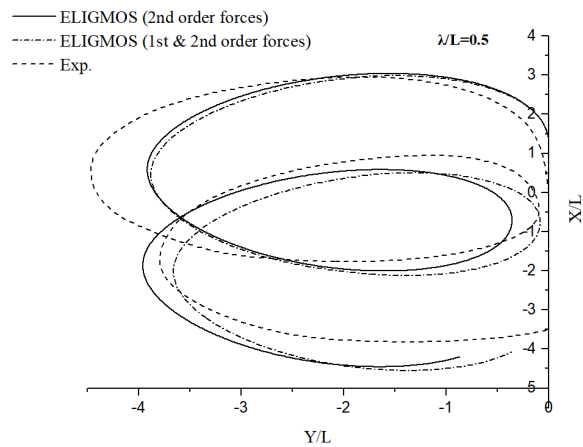


Figure 11. Comparison of yaw rate during port and starboard turning circles in regular beam waves

4. DISCUSSION

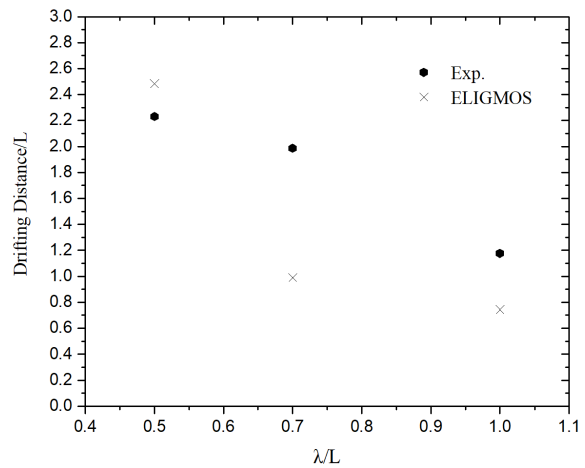
The first thing that should be mentioned here is that the incorporation of the first-order wave forces improve the results as indicated in Fig. 12, thus it is suggested that they should be taken into consideration in relevant simulations.

Additionally, in most of the cases and specifically when $\lambda/L=0.5$ or $\lambda/L=1.0$, results derived by use of ELIGMOS agree satisfactorily with the experimental ones (except for the case of ship turning to starboard in long beam waves).



$\lambda/L=0.5$

This is attributed to the fact that the added resistance for the medium wavelength ($\lambda/L=0.7$) has been calculated by adopting a near-field direct pressure integration as in case of long waves. The implementation of the far-field method when $\lambda/L=0.7$ as well, would be of great interest for future work. The aforementioned observation can be also verified by the following figure which shows a comparison of the drifting distance in case of port turning circles in head waves (Fig. 13). Ueno et al. (2003) firstly introduced this type of comparison in order to validate the efficacy of a numerical method that simulates ship's manoeuvring performance in waves. The traditional approach of comparing the major turning circle characteristics (i.e. advance, transfer and tactical diameter) is inappropriate as a steady state of the turning motion during the first 180° has not been established yet (Kim et al., 2018).



Further, the acceptable agreement of the time histories of surge and yaw velocities depicted

in Figs. 6, 7 and 10, 11 prove that the numerical solution is able to replicate the motion characteristics.

At this point, it is important to note that the values of the added masses (M_x , M_y) and added moment of inertia (J_{zz}) have been calculated at infinite wave frequency in order to account for the presence of the waves (experimentally determined zero frequency values have been considered in case of calm water manoeuvring). In the literature there isn't common ground yet regarding this issue as some researchers (e.g. Ghillece and Moctar, 2018) use the zero frequency values also in case of turning manoeuvring in a wavy environment, whilst others (e.g. Fang, 2005) consider the alteration of the hydrodynamic coefficients with respect to the encounter frequency.

CONCLUSION

In this paper, the mathematical formulation of a time-domain software (ELIGMOS) is presented that is capable of simulating a marine vessel's manoeuvring performance in regular waves. Wave impact has been modelled through the consideration of first and steady second-order forces. These forces have been incorporated in the time-domain solution through a novel multidimensional interpolation scheme. Comparison with experimental results was proved promising, especially in short ($\lambda/L=0.5$) and long ($\lambda/L=1.0$) waves. Further investigation is suggested in the medium range case ($\lambda/L=0.7$), whilst a next step forward should allow for the consideration of large waves. Additionally, a sensitivity analysis of the multidimensional interpolation scheme is suggested concerning the number of heading angle and speed input values.

ACKNOWLEDGMENTS

Dr. Boulougouris greatly acknowledges the funding from DNV GL and RCCL for the MSRC establishment and operation. The opinions expressed herein are those of the authors and should not be construed to reflect the views of DNV GL and RCCL.

REFERENCES

- Abkowitz, M. A. (1964). *Lectures on ship hydrodynamics – Steering and maneuverability*. Lyngsby, Denmark: Hydro-og Aerodynamisk Laboratorium.
- Ayaz, Z., Vassalos, D., & Spyrou, K. J. (2006). Manoeuvring behaviour of ships in extreme astern seas. *Ocean Engineering*, 33, 2381-2434.
- Chroni, D., Liu, S., Plessas, T., & Papanikolaou, A. (2015). Simulation of the maneuvering behaviour of ships under the influence of environmental forces. *Towards Green Marine Technology and Transport* (pp. 111-119). Pula, Croatia: Taylor and Francis Group, London.
- Dahlquist, G., & Björck, Å. (2003). *Numerical Methods*. Dover Books on Mathematics.
- Faltinsen, O. M., Minsaas, K., Liapis, N., & Skjördal, S. O. (1980). Prediction of resistance and propulsion of a ship in a seaway. *13th Symposium of Naval Hydrodynamics*, (pp. 505-529). Tokyo, Japan.
- Fang, M. C., Luo, J. H., & Lee, M. L. (2005). A Nonlinear Mathematical Model for Ship Turning Circle Simulation in Waves. *Journal of Ship Research*, 49(2), 69-79.
- Fonseca, N., & Soares, C. G. (1998). Time-domain analysis of large-amplitude vertical ship motions and wave Loads. *Journal of Ship Research*,

- 42(2), 139-153.
- Fournarakis N., Chroni, D., Plessas, T., Liu, S., & Papanikolaou, A. (2016). Estimation of the maneuvering characteristics of the DTC containership using URANS based simulations. *3rd International Conference on Marine Technology and Engineering* (pp. 259-268). Lisbon, Portugal: Taylor and Francis Group, London.
- Ghillece, G., & Moctar, O. (2018). A numerical method for manoeuvring simulation in regular waves. *Ocean Engineering*, 170, 434-444.
- Hirano, M., Takaishi, Y., & Saruta, T. (1980). Ship turning trajectory in regular waves. *Transactions of the West-Japan Society of Naval Architects*, 60, 17-31.
- Kim, Y. G., Lee, G. J., Nam, B. W., Seo, M. K., Kim, D. J., Yeo, D. J., & Yun, K. (2018). Simplified maneuvering simulation of a ship in waves. *Proceedings of the Asian Conference on Maritime System and Safety Research*, (pp. 29-36).
- Liu, S., Papanikolaou, A., & Zaraphonitis, G. (2011). Prediction of added resistance of ships in waves. *Ocean Engineering*, 38, 641-650.
- Maruo, H. (1960). The drift of a body floating on waves. *Journal of Ship Research*, 4(3), 1-10.
- Maruo, H. (1963). Resistance in waves. *60th Anniversary Series. The Society of Naval Architects of Japan*, 8, 67-102.
- Papanikolaou, A. (1985). On Integral-Equation Methods for the Evaluation of Motions and Loads of Arbitrary Bodies in Waves. *Journ. Ingenieur-Archiv*, 55, 17-29.
- Papanikolaou, A., & Zaraphonitis, G. (1987). On an Improved Method for the Evaluation of Second Order Motions and Loads on 3D Floating Bodies in Waves. *Schiffstechnik*, 34, 170-211.
- Papanikolaou, A., & Schellin, T. E. (1992). A Three-Dimensional Panel Method for Motions and Loads of Ships with Forward Speed. *Ship Technology Research*, 39, 147-156.
- Pollalis, C., Boulougouris, E. (2021). Time-domain simulation of the manoeuvring performance of ships in regular waves and shallow water. *1st International Conference on the Stability and Safety of Ships and Ocean Vehicles, Virtual*.
- Sano, M., & Yasukawa, H. (2008). Maneuvering Motions of KVLCC1 and KVLCC2 using MMG model. *SIMMAN, Part E*, (pp. 51-55).
- Seo, M. G., & Kim, Y. (2011). Numerical analysis on ship maneuvering coupled with ship motion in waves. *Ocean Engineering*, 38, 1934-1945.
- Skejic, R., & Faltinsen, O. M. (2008). A unified seakeeping and maneuvering analysis of ship in regular waves. *Journal of Marine Science and Technology*, 13, 371-394.
- Subramanian, R., & Beck, R. F. (2015). A time-domain strip theory approach to maneuvering in a seaway. *Ocean Engineering*, 104, 107-118.
- Sutulo, S., & Soares, C. G. (2006). Numerical Study of Ship Rolling in Turning Manoeuvres. *Proceedings of STAB 2006*.
- Ueno, M., Nimura, T., & Miyazaki, H. (2003). An experimental study on manoeuvring motion of a ship in waves. *Proceedings of the International Conference on Marine Simulation and Ship Maneuverability (MARSIM'03)*.
- Yao, J., Zuyuan, L., Xuemin, S., & Yan, S. (2021). Pure low-frequency and pure high-frequency ship motion equations in regular waves. *Ocean Engineering*, 233.

- Yasukawa, H. (2006). Simulations of ship maneuvering in waves. *Journal of the Japan Society of Naval Architects and Ocean Engineers* 4, 127–136.
- Yasukawa, H., & Nakayama, Y. (2009). 6-DOF motion simulations of a turning ship in regular waves. *International Conference on Marine Simulation and Ship Maneuverability MARSIM*. Panama City, Panama.
- Yasukawa, H., & Yoshimura, Y. (2015). Introduction of MMG standard model for ship maneuvering predictions. *Journal of Marine Science and Technology*, 20(1), 37-52.
- Zhang, W., Zou, Z., & De-Heng, D. (2017). A study on prediction of ship maneuvering in regular waves. *Ocean Engineering*, 137, 367-381.